Surface & Coatings Technology xxx (2017) xxx–xxx

Contents lists available at ScienceDirect

Surface & Coatings Technology

journal homepage: www.elsevier.com/locate/surfcoat

Effect on optical properties and electrical performances of antireflective coating with gradient refractive index based on p-type amorphous SiO_x thin films

Lu Huang *, Qi Jin, Xingling Qu, Jing Jin, Weiguang Yang, Linjun Wang, Weimin Shi

School of Materials Science and Engineering, Shanghai University, Shanghai 200444, China

ARTICLE INFO

Article history:
Received 5 August 2016
Revised 19 January 2017
Accepted in revised form 29 January 2017
Available online xxxx

Keywords:
Amorphous silicon oxide
Boron doping
Antireflective coating
Gradient refractive index
Electrical performance

ABSTRACT

The electrical performances and optical properties of p-type amorphous silicon oxide (p-SiO_x) thin films with gradient refractive index are studied. The composite thin films as antireflective coatings (ARCs) are widely used in solar cells and microelectronic devices. The double-layer p-SiO_x thin films are deposited by plasma-enhanced chemical vapor deposition (PECVD) system. To obtain better optical properties, the refractive index of ARCs can be adjusted by SiH_4 to N_2O ratio. And the electrical performances of composite thin films can be improved by adjustment of B_2H_6 to SiH_4 ratio. The computational model is built to predict the optimized range of reflection spectra corresponding to structure of p-SiO_x ARCs with gradient refractive index by finite difference time domain (FDTD) method. It shows the difference of reflection spectra with gradient refractive index distribution. The optimized reflection spectra simulated by FDTD method confirms to agree well with that measured by UV–visible spectroscopy.

1. Introduction

Nowadays amorphous silicon oxide (α-SiO_x) thin films on glass substrates have attracted a great deal of attention in photovoltaics, microelectronics and display technologies because of its potential applications for electronic devices, especially amorphous silicon (α-Si) thin film solar cells [1–3]. Excellent solar cells must satisfy two kinds of requirements in optical properties (strongly optical absorption) and electrical performances (effectively electrical transportation and lower leakage current). Therefore antireflective coatings (ARCs) have been widely used in manufacturing process of conventional crystalline solar cells (c-Si) to benefit optical absorption, such as silicon nitride (Si_xN_y) [4–5] and aluminum oxide (Al_xO_y) prepared on the surface of n-type and p-type c-Si respectively [6–7]. Compared to c-Si solar cells, oxide layers are also selected to deposit on the surface of α-Si thin films to obtain better antireflective effect [8–9]. The p-type amorphous silicon oxide (p-SiO_x) thin films are prepared as conductive ARCs by plasma-enhanced chemical vapor deposition (PECVD) [10–11], magnetron sputtering [12–13] and sol-gel methods [14–16] because of the match of lattice to α-Si substrates. However it is more suitable to prepare composite films with different refractive index by PECVD system. Because single-layer ARC has only minimal point of reflectance, the average reflectance for double-layer ARCs is lower over a broader wavelength range than single-layer ARC [17–18]. With these requirements, double-layer p-SiO_x ARCs with gradient refractive index not only decrease electrical recombination and leakage current effectively, but also enhance optical antireflection and ohmic contact strongly [19–21].

In this paper, compared to conventional p-α-Si layer, the composite p-SiO_x thin films not only decrease optical reflectance, but also improve electrical conductivity. The high doping conductive layer can enhance ohmic contact with metallic electrode, and the low doping passivated layer can decrease leakage current of device. Reflection spectra of double-layers p-SiO_x ARCs with gradient refractive index are simulated by finite difference time domain (FDTD) method. The characterization of UV–visible spectroscopy aims to focus on the correlation between reflection spectra and gradient refractive index distribution. However, it is worth investigating how to enhance antireflective and conductive effect of α-Si thin film solar cells through different composite structures of p-SiO_x ARCs.

2. Experimental and computational details

The p-SiO_x thin films were prepared by the following procedure. Firstly, the substrate was pretreated by pure argon (Ar_2) plasma at working pressure of 0.4 Torr and flow ratio of 30 sccm. Secondly, the p-SiO_x:H films as a layer was deposited on the glass substrates using PECVD by silane (SiH_4), nitrous oxide (N_2O), diborane (B_2H_6) and hydrogen (H_2). The pressure of deposited p-SiO_x:H thin films inside the chamber was 0.6 Torr and the temperature on substrates was kept at 200 °C. The RF frequency and power for depositing thin film was 13.56 MHz and 80 W respectively. The PECVD system is HLF-400 made in Beijing Beiyi Innovation Vacuum Technology Co. Ltd. Before the thin films were deposited on glass substrate, heat-resistant tape

* Corresponding author.
E-mail address: lhuang@shu.edu.cn (L. Huang).

http://dx.doi.org/10.1016/j.surfcoat.2017.01.110
0257-8972/

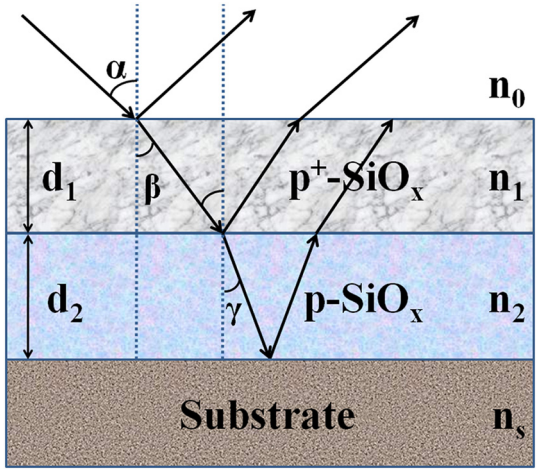

Fig. 1. The basic cross-section structures of double p-SiO_x ARCs on the substrate.

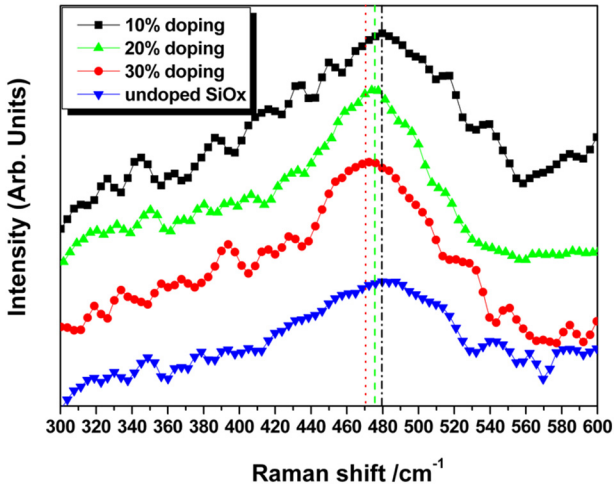

Fig. 2. The characterization of Raman spectra for sample a, b, c and d.

had been adhered to the corner of glass substrate. After we finished depositing p-SiO_x:H thin films and uncover tape from the substrate, the thickness of thin film was measured on the step between glass substrate and thin films by stylus profiler. Thickness measurement of stylus profiler is Surfcorder ET 150. Then double-layer structures were formed on the surface of first layer according to above procedure again. Thirdly, all of samples had been dehydrogenated after thin films were annealed in vacuum condition at 200 °C for 30 min. Finally, the silver electrode was deposited on the surface of thin films to form good ohmic contact using DC magnetron sputtering. The DC power of sputtering was about 100 W at working gas of pure Ar_2. The magnetron sputtering system is JPGF-400A made in Beijing Beiyi Innovation Vacuum Technology Co. Ltd.

The structural orientation of p-SiO_x films were measured by Jobin Yvon LabHR Raman spectrometer at room temperature using the 514.5 nm line of an Ar + laser. The cross-section morphology and element composition of thin films was characterized respectively by scanning electron microscope (SEM) and energy dispersive spectrometer (EDS) made by JEOL JSM-6700F. The refractive index was measured by spectroscopic ellipsometer of Sentech SE-400adv. UV–visible reflection spectra were performed by Hitachi U-2910 spectrophotometer. The electrical performances including dark conductivity were tested by Keithley 4200.

In this computational model, the software of FDTD Solution is used as analysis for simulating different composite structures of p-SiO_x ARCs with gradient refractive index. The size of rectangular model is that the length, width and height are 2.5 μm, 2.5 μm and 0.1 μm respectively. The physical and optical values of silicon oxide materials are used as parameters in the simulation. Different structures of p-SiO_x ARCs with gradient refractive index are selected to simulate the properties of optical reflection. The optimal results can be analyzed to obtain the lowest average reflectance in the wavelength range of visible light. The basic cross-section structures of double-layer p-SiO_x thin films on the substrate have been shown in Fig. 1.

The reflectance of double-layer structures has either a minimum or a local maximum for quarter wavelength optical films ($n_1d_1 = n_2d_2 = \lambda_0/4$). This reflectance is given by Eq. (1):

$$R = \left[\left(n_1^2 n_s - n_0 n_2^2\right)/\left(n_1^2 n_s + n_0 n_2^2\right)\right]^2 \quad (1)$$

which R approaches zero if the condition meets $n_2^2/n_1^2 = n_s/n_0$, and approaches a local maximum with zero reflectance on either side if the condition meets $n_1 n_2 = n_0 n_s$. Therefore the average reflectance for double ARCs are lower over a broader wavelength range than for a single ARC, because single ARC has only minimal value of reflectance [22].

3. Results and discussion

3.1. Morphology and structure

We select eleven kinds of samples deposited by different gas ratio of B_2H_6, SiH_4 to N_2O, such as 0:1:1, 0.1:1:1, 0.2:1:1 and 0.3:1:1

Table 1
The refractive index, dark conductivity and thickness of p-SiOx ARC samples for different gas ratio.

Sample no.	B_2H_6: SiH_4: N_2O: H_2 (Vol%)	Refractive index	Conductivity (S * cm^{-1})	Thickness (nm)
a	0:10:10:100 (0:1:1:10)	2.267	$8.86 * 10^{-10}$	84.6
b	1:10:10:100 (0.1:1:1:10)	2.282	$9.65 * 10^{-9}$	83.8
c	2:10:10:100 (0.2:1:1:10)	2.303	$7.54 * 10^{-8}$	86.5
d	3:10:10:100 (0.3:1:1:10)	2.295	$1.38 * 10^{-7}$	91.4
e	Outer layer: 3:10:10:100 (0.3:1:1:10) Inner layer: 1:10:5:100 (0.1:1:0.5:10)	2.322	$9.78 * 10^{-6}$	114.6
f	Outer layer: 3:10:20:100 (0.3:1:2:10) Inner layer: 1:10:5:100 (0.1:1:0.5:10)	2.287	$1.26 * 10^{-7}$	112.4
g	Outer layer: 3:10:30:100 (0.3:1:3:10) Inner layer: 1:10:5:100 (0.1:1:0.5:10)	2.165	$1.94 * 10^{-7}$	107.2
h	Outer layer: 3:10:20:100 (0.3:1:2:10) Inner layer: 1:10:10:100 (0.1:1:1:10)	2.193	$2.57 * 10^{-7}$	108.7
i	Outer layer: 3:10:30:100 (0.3:1:3:10) Inner layer: 1:10:20:100 (0.1:1:2:10)	1.875	$3.25 * 10^{-7}$	98.9
j	Outer layer: 2:10:30:100 (0.2:1:3:10) Inner layer: 1:10:10:100 (0.1:1:1:10)	2.064	$8.63 * 10^{-8}$	111.8
k	Outer layer: 3:10:30:100 (0.3:1:3:10) Inner layer: 1:10:10:100 (0.1:1:1:10)	2.097	$1.41 * 10^{-7}$	110.2

Please cite this article as: L. Huang, et al., Surf. Coat. Technol. (2017), http://dx.doi.org/10.1016/j.surfcoat.2017.01.110

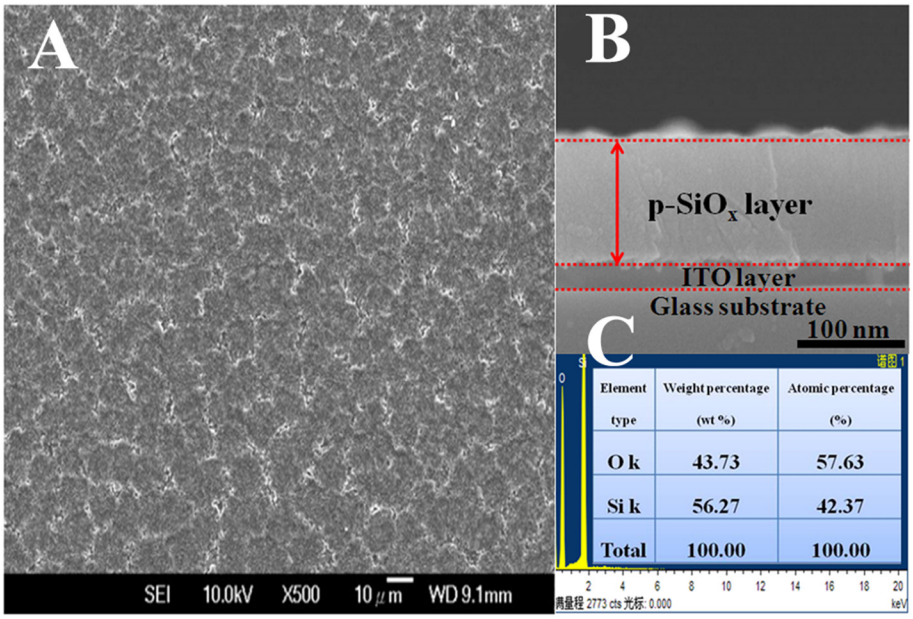

Fig. 3. (A) The surface morphology of sample k characterized by SEM (B) The cross-section structure of sample k characterized by SEM (C) The weight and atomic percentage of element for sample k characterized by EDS.

respectively, to investigate the surface and cross-section morphology of thin films. The related experimental parameters of samples for single- and double-layer films have been shown in Table 1.

The characterization of Raman spectra is also displayed in Fig. 2. The undoped i-SiO_x and p-SiO_x phase can be obtained through different peak shift. The i-SiO_x exhibits a broad peak at ~480 cm^{-1} (sample a in Fig. 2). Because i-SiO_x thin films are still amorphous phase, the broad transverse optical (TO) phonon peak at ~480 cm^{-1} demonstrates amorphous phase. When the ratio of B_2H_6 in mixed gas is increased, the blueshift of Raman peak for p-SiO_x indicates the presence of stress in doped films. The effect of stress on Raman spectra for p-SiO_x originates from the lattice deformation, which leads to modified frequencies of the optical phonons. The empirical equation on in-plane stress of thin film layer is given by [23]

$$\sigma(\mathrm{GPa}) = -0.2 * \Delta\omega_{TO}(\mathrm{cm}^{-1}) \quad (2)$$

where $\Delta\omega_{TO}$ stands for the frequency shift of TO Raman signal at 480 cm^{-1}. Following this reasoning, compressive stress results in a blueshift to the Raman shift, while tensile stress induces a redshift. Therefore, the effect of blueshift for p-SiO_x can be observed in characterization of Raman spectra (sample b, c and d in Fig. 2). When silicon atoms are substituted for boron atoms by B_2H_6 doping, the primitive cell trends to obtain compressive stress because the atom radius of boron is shorter than that of silicon. We can obtain the frequency shift of Raman peak in 470.4 cm^{-1}, 475.2 cm^{-1} and 479.4 cm^{-1}corresponding 30%, 20% and 10% doping. The quantitative assessment of stresses is calculated about 1.92 GPa, 0.96 GPa and 0.12 GPa corresponding to 30%, 20% and 10% doping samples by Eq. (2).

The surface and cross-section SEM image of sample k has been demonstrated in Fig. 3(A) and Fig. 3(B) respectively, indicating that the roughness on surface of p-SiO_x film is low and the film thickness of sample k is about 110 nm. The double p-SiO_x ARCs have been deposited on the glass substrate coating Sn_2O_3:In transparent conductive oxide (ITO), because SiO_x layer and glass substrate can be separated obviously by ITO layer from SEM image. The atomic ratio of element O to Si is about 57.63/42.37 = 1.36, which is characterized by EDS analysis in Fig. 3(C). Because the atomic weight of boron is too low and the doping concentration is lower than 1%, the atomic ingredient only includes Si and O atoms and not B atoms in Fig. 3(C). As a result, sample k is proven to be the best condition of SiO_x ARC with gradient refractive index, which can also be confirmed by optical results experimentally and numerically later.

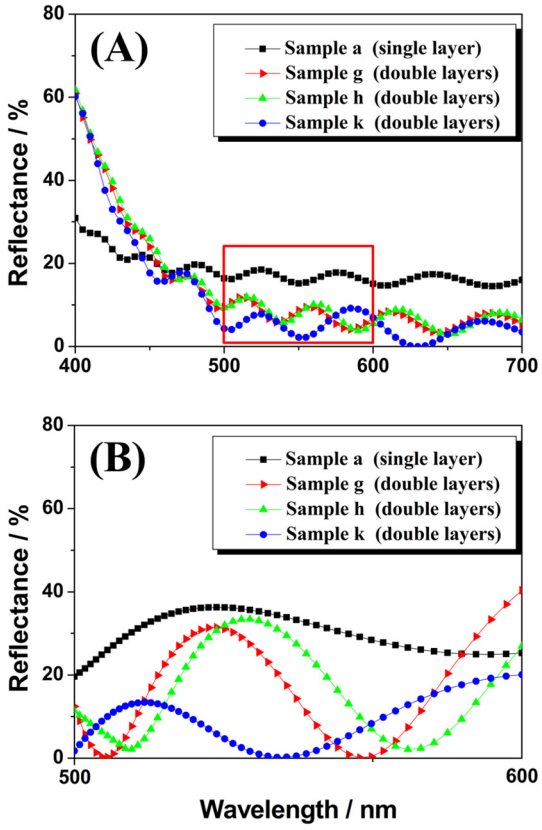

Fig. 4. (A) UV–visible reflection spectra and (B) FDTD simulative reflection spectra of sample a, g, h and k.

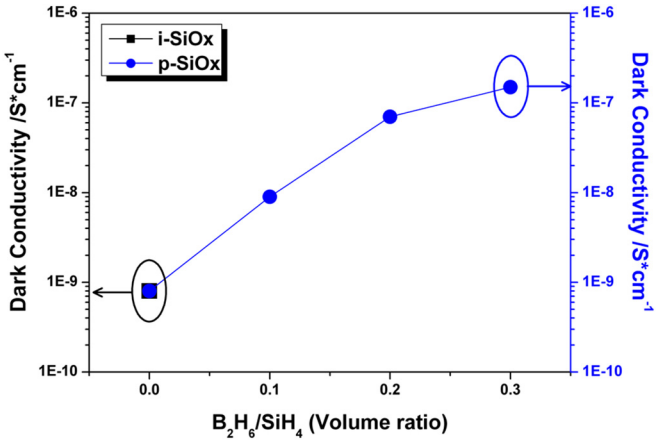

Fig. 5. The dark conductivities of p-SiO_x thin films doped by B_2H_6 in different volume ratio (from 0% to 30%).

3.2. Optical properties

The refractive indexes of p-SiO_x thin films measured by spectroscopic ellipsometer have been listed in Table 1. When the ratio of SiH_4 in mixed gas is increased, the velocity of growth for p-SiO_x thin film becomes faster and the value of refractive index for thin film becomes higher. It is found that the gradient refractive index of p-SiO_x ARCs can be obtained by adjustment of SiH_4 to N_2O ratio.

In the structure of SiO_x ARCs on the substrate, the reflection spectra are analyzed by FDTD simulation. The reflection spectra are assumed to vary through different refractive index of single and double layer thin film. It is proved theoretically that the correlation between reflection spectra and gradient refractive index distribution can be obtained from FDTD simulation. Meanwhile the reflection spectra of p-SiO_x ARCs with gradient refractive index are deduced from the UV–visible spectrophotometer. We obtained reflection spectra by UV–visible spectral characterization as illustrated in Fig. 4(A) and FDTD simulation as shown in Fig. 4(B). The reflection spectra corresponding to sample a, g, h and k have been displayed in Fig. 4 respectively.

To obtain lowest average reflectance (<10%), the best ratio of gradient refractive index for double ARCs must meet Eq. (1). When the substrate is silicon material ($n_{si} = 3.9$), the optimized value of refractive index for single ARC is about 2. The simulative result is a little difficult to match the experimental result completely, such as different parameters of processing and roughness on surface of thin films shown in Fig. 3(A). For above reasons, It is found that sample k is optimized double ARCs with gradient refractive index in a broader wavelength range compared to other samples. Therefore the reflection spectra simulated by FDTD method in Fig. 4(B) accords very well to the experimental result characterized by UV–visible spectrophotometer in Fig. 4(A), especially in wavelength range from 500 nm to 600 nm.

3.3. Electrical performances

The dark conductivities of the undoped i-SiO_x and p-SiO_x thin films are shown in Fig. 5. It is found that the conductivity of the p-SiO_x thin films, which is higher than undoped i-SiO_x thin films. It illustrates that the dark conductivities of amorphous SiO_x thin films have been improved by doping diborane. The conductivity is also compared with different volume ratio of doping B_2H_6. When the volume ratio of doping B_2H_6 is increased from 0% to 30%, the conductivities of thin films are about $8.86 \times 10^{-10}\ S * cm^{-1}$, $9.65 \times 10^{-9}\ S * cm^{-1}$, $7.54 \times 10^{-8}\ S * cm^{-1}$ and $1.38 \times 10^{-7}\ S * cm^{-1}$ respectively. It can be explained that the conductivity of p-SiO_x thin film can be increased with the improvement of doping B_2H_6 ratio properly. The high doping outer layer can enhance ohmic contact with metallic electrode, and the low doping inner layer can decrease leakage current of device. And the electrical performances of composite thin films can be improved by adjustment of B_2H_6 to SiH_4 ratio.

4. Conclusions

In this paper, the single- and double-layer structures of p-SiO_x ARCs with gradient refractive index are investigated experimentally and theoretically. The computational model is used to predict the optimal reflection spectra corresponding to double ARCs structure of gradient refractive index by FDTD method. The lowest average reflectance (<10%) in broader wavelength range is achieved by optimized gas ratio of B_2H_6, SiH_4 to N_2O (outer layer 0.3:1:3, inner layer 0.1:1:1) in the experiment. The optical simulation accords very well to optical characterization of thin films with gradient refractive index. The dark conductivity of composite thin films can be improved to ~$10^{-7}\ S * cm^{-1}$ by adjustment of doping B_2H_6 ratio.

Acknowledgments

The authors gratefully acknowledge the financial support of the project funded by the Special Research Foundation for Training and Selecting Outstanding Young Teachers of Universities in Shanghai (no. ZZSD16011), National Science Foundation of China (Grant no. 61404080 and 51202139). They also thank Mr. Yuliang Chu (Analysis and Testing Center of Shanghai University) for their kind assistance with FESEM measurements.

Reference

[1] G. Fortunato, Thin Solid Films 296 (1997) 82.
[2] A.H. Mahan, Sol. Energy Mater. Sol. Cells 78 (2003) 299.
[3] S.D. Brotherton, Semicond. Sci. Technol. 10 (1995) 721.
[4] S. Duttagupta, F.J. Ma, B. Hoex, A.G. Aberle, Sol. Energy Mater. Sol. Cells 120 (2014) 204.
[5] Q. Qiao, H.Y. Lu, J. Ge, X. Xi, R.L. Chen, J. Yang, J.B. Zhu, Z.R. Shi, J.H. Chu, Appl. Surf. Sci. 305 (2014) 439.
[6] H. Lee, T. Tachibana, N. Ikeno, H. Hashiguchi, K. Arafune, H. Yoshida, S.I. Satoh, T. Chikyow, A. Ogura, Appl. Phys. Lett. 100 (2012) 143901.
[7] T. Dullweber, C. Kranz, B. Beier, B. Veith, J. Schmidt, B.F.P. Roos, O. Hohn, T. Dippell, R. Brendel, Sol. Energy Mater. Sol. Cells 112 (2013) 196.
[8] A. Lambertz, T. Grundler, F. Finger, J. Appl. Phys. 109 (2011) 113109.
[9] J.P. Seif, A. Descoeudres, M. Filipic, F. Smole, M. Topic, Z.C. Holman, S.D. Wolf, C. Ballif, J. Appl. Phys. 115 (2014) 024502.
[10] L. Remache, E. Fourmond, A. Mahdjoub, J. Dupuis, M. Lemiti, Mater. Sci. Eng., B 176 (2011) 45.
[11] Z.Z. Chen, P. Sana, J. Salami, A. Rohatgi, IEEE Trans. Electron Devices 40 (1993) 1161.
[12] B. He, H.Z. Wang, Y.G. Li, Z.Q. Ma, J. Xu, Q.H. Zhang, C.R. Wang, H.Z. Xing, L. Zhao, Y.C. Rui, J. Alloys Compd. 581 (2013) 28.
[13] W.B. Qiu, Y.H. Ma, J. Zhao, J.X. Wang, M.K. Li, S.Y. Li, J.Q. Pan, Jpn. J. Appl. Phys. 53 (2014) 021501.
[14] N. Iari, S. Ahangarani, A. Shanaghi, J. Mater. Eng. Perform. 24 (2015) 2645.
[15] S.Y. Lien, D.S. Wuu, W.C. Yeh, J.C. Liu, Sol. Energy Mater. Sol. Cells 90 (2006) 2710.
[16] H.Y. Li, H. Xiong, Y.X. Tang, L.L. Hu, Rare Metal Mater. Eng. 39 (2010) 145.
[17] J.J. Liu, W.J. Ho, Y.Y. Lee, C.M. Chang, Thin Solid Films 570 (2014) 585.
[18] D.Z. Li, D.Y. Wan, X.L. Zhu, Y.M. Wang, Z. Han, S.S. Han, Y.K. Shan, F.Q. Huang, Sol. Energy Mater. Sol. Cells 130 (2014) 505.
[19] R. Xu, X.D. Wang, L. Song, W. Liu, A. Ji, F.H. Yang, J.M. Li, Opt. Express 20 (2012) 5061.
[20] D.Y. Kim, E. Guijt, F.T. Si, R. Santbergen, J. Holovsky, O. Isabella, R.A.C.M.M.V. Swaaij, M. Zeman, Sol. Energy Mater. Sol. Cells 141 (2015) 148.
[21] J. Park, C. Shin, S. Lee, S. Kim, J. Jung, N. Balaji, V.A. Dao, Y.J. Lee, J. Yi, Thin Solid Films 587 (2015) 132.
[22] H.J. Hovel, Semiconductors and semimetals, Solar Cells, 11, Academic Press, USA, 1975.
[23] I.D. Wolf, Semicond. Sci. Technol. 11 (1996) 139.